Med Discoveries
An open access journal of science and medicine

Article Type: Research Article
Volume 2, Issue 11
Received: Oct 31, 2023
Accepted: Nov 21, 2023
Published Online: Nov 28, 2023

Identification of Comparative Collagen Fibril Associated Changes in Normal and Keratoconus Corneas using Vibrational Optical Coherence Tomography and Machine Learning

Frederick H Silver[1,2]*; Dominick Benedetto[3]; Tanmay Deshmukh[2]; Nathalie A Daher[4]

[1]Department of Pathology and Lab Medicine, Rutgers, The State University of New Jersey, Piscataway, NJ 08854, USA.

[2]Optovibronex, LLC, Ben Franklin Tech Ventures, Bethlehem, PA 18015, USA.

[3]Center for Advanced Eye Care, Vero Beach FL 32960, USA.

[4]Cornea Service, Wills Eye Hospital, Philadelphia, PA 19104, USA.

***Corresponding Author:** Frederick H Silver*

Email: silverfr@rutgers.edu

Abstract

Vibrational Optical Coherence Tomography (VOCT) is a non-invasive technique that uses infrared light and audible sound to characterize tissues noninvasively. We have used VOCT in vivo to characterize the differences between control corneas and corneas with stages I, II, III and IV Keratoconus (KC). VOCT studies comparing control normal corneas to corneas from KC patients suggest that changes are observed in the collagen deposited in the limbus and lamellae that lead to changes in the average elastic modulus (stiffness). Normal average central corneal modulus values are significantly higher than the values for KC corneas. However, the average modulus values of inferior KC corneas are statistically higher than those for normal corneas. VOCT and machine learning results are consistent with the loss in stiffness occurring in the KC central regions. The loss in the average elastic modulus in the central region is observed to be compensated by an increase in the component moduli and average modulus in the inferior KC cornea. This suggests that the loss in KC average central/paracentral corneal modulus leads to cone formation at a point where the radius of curvature is largest due to stress concentration. The results of pilot machine learning studies using a logistic regression model indicate that differences in the 140-150 and 240-250 Hz resonant frequency peaks can be used to differentiate between controls and stages I, II, III, and IV KC corneas with a sensitivity and specificity of above 90%. Determination of the exact sensitivity and specificity will require additional data on KC subjects but the agreement between the machine learning results and the statistical analysis of the VOCT data suggest that KC corneas of different stages can be clinically identified using VOCT.

Keywords: Cornea; Limbus; Elastic modulus; Stiffness; Viscoelasticity; Bowman's layer; Epithelium; Collagen.

Citation: Silver FH, Benedetto D, Deshmukh T, Daher NA. Identification of Comparative Collagen Fibril Associated Changes in Normal and Keratoconus Corneas using Vibrational Optical Coherence Tomography and Machine Learning. Med Discoveries. 2023; 2(11): 1093.

Introduction

Energy storage, transmission, and dissipation are important functions of all mammalian tissues that promote locomotion and movement and also protect against premature mechanical failure of tissues [1-5]. Results of a recent study suggest that the porcine corneal-limbus-scleral biomechanical unit stores mechanical energy applied to the eye during loading and is postulated to transmit some of the energy through the sclera to the posterior segment of the eye [6]. This transfer of applied energy from the cornea to the posterior segment of the eye prevents the cornea from delamination, buckling, and cone formation under applied loads [6]. The loss of energy storage and transmission by the cornea may lead to cone formation and eventual mechanical failure in diseases such as keratoconus and corneal ectasia.

Keratoconus (KC) is a progressive corneal disease characterized by thinning and steepening of the cornea, often leading to visual impairment due to astigmatism and scarring [7]. Keratoconus appears positively associated with multiple immune-mediated diseases and systemic inflammatory responses have been proposed to influence its onset [8]. Progressive stromal thinning, rupture of the anterior limiting membrane, and subsequent ectasia of the central/paracentral cornea are common histopathological findings [9]. Mild to moderate cases of progressive KC are treated surgically, most commonly with corneal crosslinking [9] although insertion of intrastromal rings is also reported for mild to moderate disease [10]. Historically, penetrating keratoplasty (corneal transplantation) has been the standard of care in the surgical management in keratoconus for very thin corneas.

Histopathological, chemical, and mechanical observations on KC corneas have been reported as well as changes that are observed when compared to normal tissues [11-16]. KC results in corneal protrusion, irregular astigmatism, and decreased vision [11,13]. With subsequent disease progression, the KC cornea assumes an irregular conical shape because of the changes to corneal stromal tissue and the subsequent normal tensile forces that pull the cornea away from the point of initiation. Morphological changes in collagen fibers, such as interlamellar displacement and slippage, may explain stromal thinning in KC eyes [12]. Significant alterations in various biochemical factors such as extracellular matrix components, cellular homeostasis regulators, inflammatory factors, hormones, metabolic products, and chemical elements have been reported in KC [17]. In KC patients, corneal biomechanical indices are correlated with corneal tomographic parameters [18]. It has been hypothesized that biomechanical alterations in KC patients can be detected before morphologic changes. Biomechanics of KC has been investigated only indirectly to a limited extent due to lack of in vivo measurement techniques and/or devices [19].

Research on corneal diseases has focused on measuring corneal biomechanical parameters in vivo using two commercially available instruments: The Ocular Response Analyzer (ORA) and the Corvis ST (CST) [13]. The data generated with these instruments use differences in the testing parameters that do not directly measure the corneal stiffness [13]. Studies using these instruments have reported significant differences between KC and healthy corneas; however, neither instrument can currently be used to reliably diagnose KC [13]. While these studies are important in identifying changes in corneal properties that occur in KC, they fail to identify the pathobiological changes to specific anatomic components and regions that are involved in early diagnosis of the disease.

Vibrational Optical Coherence Tomography (VOCT) is a non-invasive method that has been used to study the viscoelasticity of the anterior segment of both human and porcine eyes [6,20,21]. VOCT results indicate that corneal tissues are highly viscoelastic and can dissipate large amounts of applied energy that limit mechanical changes occurring in the anterior segment of the eye [6]. It has been proposed that a relationship exists between energy storage and transmission of the cornea-limbus-scleral series biomechanical unit and the mechanical stability of the cornea in vivo [6]. This relationship limits structural changes in the cornea and protects against acute or chronic insult.

VOCT has been used to evaluate the resonant frequency and elastic modulus of the components of human eyes [6,20-21], whole porcine eyes, and excised porcine eye components [6]. Studies have been conducted to identify the ocular components responsible for the cellular resonant frequency peaks at 60 to 80 Hz (epithelia and keratocytes), collagenous lamellar peaks at 110-120 Hz and 150-160 Hz, and the corneal limbus collagen peak at 240-250 Hz in pig eyes and in humans [6,20-21].

A variety of forces act on the corneal-limbus-scleral unit, including atmospheric pressure, gravity, lid pressure, intraocular pressure, muscular forces, and surface tension from the tear film [6]. These internal and external forces give rise to tension that stretches the cornea across the front of the eye. At mechanical equilibrium, all external and internal biomechanical forces acting on the cornea must be balanced, or the connection between the cornea and limbus will elongate and may lead to tearing and cone formation.

The purpose of this paper is to present the results of a pilot study to compare the resonant frequency and elastic moduli of cells and collagen in normal subjects and in subjects diagnosed with stages I, II, III and IV KC. VOCT results presented below suggest that the normal central cornea and inferior cornea have different average elastic moduli in controls; in KC patients these moduli are different than those found for the control eyes.

Materials and methods

Mechanovibrational VOCT spectra were collected on 41 normal control eyes and 22 eyes from subjects diagnosed with stages I, II, III, and IV KC after IRB approval from Wills Hospital was obtained and patients gave their informed consent as previously described (Table 1) [20]. Eyes from patients exhibiting the following stages of KC were studied: Stage I (N=2), stage II (N=9), stage III (3), and stage IV (8). None of the patients underwent collagen crosslinking prior to making the VOCT measurements. Measurements were made by focusing the IR beam centrally and then on the inferior cornea above the limbus (at 6 o'clock) with the subject looking upward.

Table 1: Identification of the parameters used to stage KC patients in this study.

	Number of samples	Posterior radius of curvature	Thickness (mm)
Control	41	6.71 ± 0.23 mm	5.38 ± 0.39 mm
KC Stage I	2	5.80 ± 0.007 mm	5.19 ± 0.02 mm
KC Stage II	9	5.51 ± 0.179 mm	5.05 ± 0.21 mm
KC Stage III	3	5.07 ± 0.092 mm	5.06 ± 0.108 mm
KC Stage IV	8	4.29 ± 0.52 mm	4.69 ± 0.41 mm

Resonant frequency and elastic modulus measurements

VOCT is a technique that uses infrared light reflected to a detector from different depths in a tissue to create an image before and after an acoustic force is applied non-invasively [6,20-26]. By applying an acoustic force from a speaker and measuring the change in displacement of the tissue components using OCT raw images of the tissue, it is possible to calculate the component resonant frequencies and tissue component elastic moduli as well as an average elastic modulus [22-26]. A stiffer component will have a larger displacement than a softer component under a fixed sound input. To isolate the elastic response the weighted displacement of a tissue was obtained after correction for the displacement of the speaker, background noise, and out-of-phase vibrations (loss modulus) as a function of frequency.

OCT images

OCT image collection was conducted using a Lumedica Spectral Domain OQ 2.0 Labscope (Lumedica Inc., Durham, NC, USA) operating in the scanning mode at a wavelength of 840 nm. The device generates a 512x512-pixel image with a transverse resolution of 15 mm and an A-scan rate of 13,000/sec. All gray scale OCT images were color-coded to enhance the image details. The images were used to locate where the VOCT measurements were made on each patient. Special software is used to analyze single OCT raw images at a fixed position with a diameter of 0.25 mm in the sample for subsequent VOCT measurements. OCT images were color-coded to improve visualization of the epithelium and collagen fibrillar components.

The resonant frequency of a tissue component is defined as the frequency at which the maximum in-phase displacement (maximum energy storage) is observed in each tissue component in the amplitude data. The measured resonant frequencies are converted into elastic modulus values using a calibration equation (Equation 1) developed based on in vitro uniaxial mechanical tensile testing and VOCT measurements made on collagenous tissues made at the same time as reported previously [21-27]. The resonant frequency of each sample is determined by measuring the displacement of the tissue resulting from applied sinusoidal audible sound driving frequencies ranging from 50 Hz to 250 Hz, in steps of 10 Hz. Since the measurements were made at 10 Hz steps the resonant frequencies were observed to occur at intervals of +/- 10 Hz. For this reason, the location of the peaks on some of the samples differ by as much as 10 Hz. The peak frequency (the resonant frequency), f_n, is defined as the frequency at which the elastic displacement is maximized after the vibrations due to the speaker are removed.

$$E\ x\ d = 0.0651\ x\ (fn^2) + 233.16 \qquad (1)$$

Since soft tissues have a density very close to 1.0; equation (1) is valid for most soft tissues found in the body as well as for several synthetic polymers; where the thickness d is in m and is determined from OCT images. fn^2 is the square of the resonant frequency, and E is the tensile elastic modulus (stiffness) in MPa as discussed previously [21-26]. Equation (1) was used to calculate the modulus values and is an empirical equation based on calibration studies [21-23]. The elastic modulus measured using VOCT is a materials property at the resonant frequency at low strains since the viscous component of the behavior is only about 5% of the total modulus at frequencies above 100 Hz [22,23]. The modulus of soft tissues is approximately constant at strains less than about 7% (low strain region of the stress-strain curve) for collagenous materials [24-27].

The average modulus was calculated by calculating the product of the weighted displacement peak height (see Figure 1) and the component modulus values (see Figure 2) and then dividing by the sum of the peak heights. The whole average central or inferior cornea modulus is therefore an average weighted by the amount of light reflected from the individual tissue components back to the detector.

The ratio of epithelial thickness at the thinnest part of the inferior cornea to the maximum thickness at the limbus was determined from OCT images. For the epithelium thickness, the central part of the cornea OCT image was used to check the location of the thinnest portion. The corneal thickness was then measured at the limbus from the OCT images.

Statistics

All resonant frequencies and moduli were analyzed for statistical differences using a one-tailed unpaired student's t test and the differences were considered significant if the p values were less than 0.05.

Machine learning analysis for human control vs KC corneas

Machine learning models

Different machine learning models such as logistic regression, Support Vector Machine (SVM) and Decision Tree were trained to identify the differences between normal human and KC corneas. The logistic regression model was chosen to analyze the data since it provided the highest specificity and sensitivity of the results.

The datasets consisted of weighted displacement peak heights vs frequency data for the controls and KC corneas. The peak heights at each frequency from 50 Hz to 250 Hz were used in the analysis. These frequencies were used as features for the machine learning models. The dataset contained 41 control samples and 22 KC samples. Stage I, II, III and IV KC patient data sets were selected to be analyzed based on changes in the posterior radius of curvature as an indicator of KC. Because of the limited data for KC corneas, 75% of the data was used to train the model whereas the remaining 25% was used to test the prediction accuracy of the model.

True Positive (a)	False Positive (b)
False Negative (c)	True Negative (d)

Each model was tested for selected frequencies to find out which frequency contributed most to distinguishing between controls and different stages of KC. Differences in the model predictability was based on calculations including of accuracy, sensitivity, and specificity. The formulas defining these parameters are given in equations (2) through (4).

% Sensitivity = [a / (a + c)] x 100 (2)

% Specificity = [b / (b + d)] x 100 (3)

% Accuracy = (a + d) / (a + b + c + d) x 100 (4)

VOCT results

We have previously reported the use of VOCT to characterize the resonant frequencies and elastic moduli of individual components of human and porcine corneas [1,20-23]. In this study we used VOCT to compare the mechanovibrational spectra of normal and KC corneas in vivo to determine if the component

and average corneal elastic moduli are similar in different parts of the eye and whether changes occur associated with the onset of KC. Figure 1 shows a comparison between the normalized weighted displacement versus resonant frequency measurements made on the central cornea (41 control eyes) and from patients with stages I, II, III, and IV KC (22 eyes). The resonant frequency peak heights of the central corneal of control eyes at 60-80 Hz are statistically different than those of the KC eyes as well as the peaks at 140, 150, and 240-250 Hz. In Figure 1, the KC peak heights at 60-80, 140, 150, and 240-250 Hz are all significantly different at a p value of 0.05 compared to the control central corneas. The inferior component heights of 60-80, 140, 150, and 240-250 Hz peaks in KC central corneas compared to the control central corneas suggests that these peak heights can be used to distinguish between KC corneas and controls. The 140 and 150 Hz peak heights are shown separately; however, since the peak heights were measured at 10 Hz intervals there may be some overlap in these peaks.

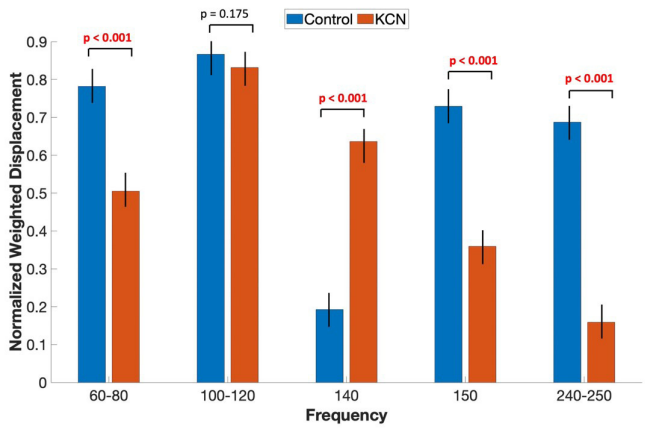

Figure 1: Normalized average weighted displacements versus frequency for control central corneas and central corneas from subjects with stages I, II, III, and IV KC. The data shown in this plot illustrates that the cellular peaks are lowered in KC (60-80 Hz peak) consistent with epithelial cell changes, the 140 peak is increased in KC (collagen), the 150 Hz peak (collagen lamellae) decreases, and the 240-250 Hz peak is much lower than controls. The 240-250 Hz has been previously shown to be associated with the limbus. There may be some overlap in the 140 and 150 Hz peaks.

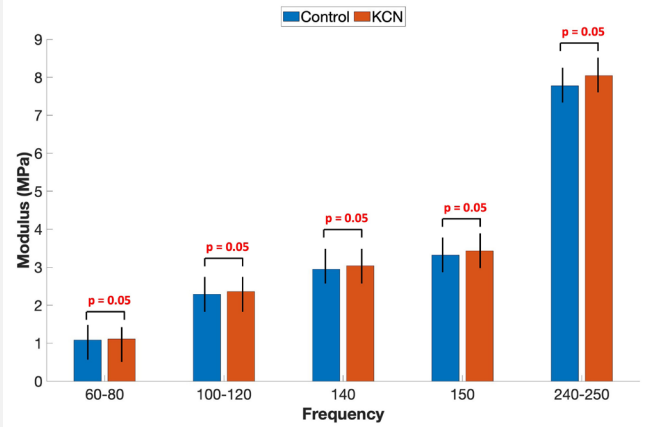

Figure 2: The average modulus of different central corneal components from controls and KC subjects calculated from resonant frequency measurements (see Figure 1) determined from VOCT testing. Note the small differences between the moduli of the components of controls and KCN subjects (Figure 2) compared to the large differences in the component peak heights seen in Figure 1. This data indicates that KC individual components are somewhat stiffer than those of control central corneas; however, the biggest difference is that normal control central corneal components contain more of the stiffer components.

Figure 2 illustrates that the moduli of the components of central KC corneas are slightly higher than those of control corneas. The moduli were calculated using equation (1). The results suggest that although the KC corneas are thinner than control corneas the modulus of the individual components are slightly higher. This suggests that the exact collagenous component amounts of control and KC corneas differ, but the component stiffnesses may not be different in KC. Results reported in Figures 1 and 2 suggest that the differences in control and KC central corneas arise from different distributions of tissue components. Figure 3 illustrates that the central cornea of controls has a significantly higher average modulus compared to subjects with stages I, II, III and IV KC primarily due to differences in the amount of the stiffer components based on Figure 1.

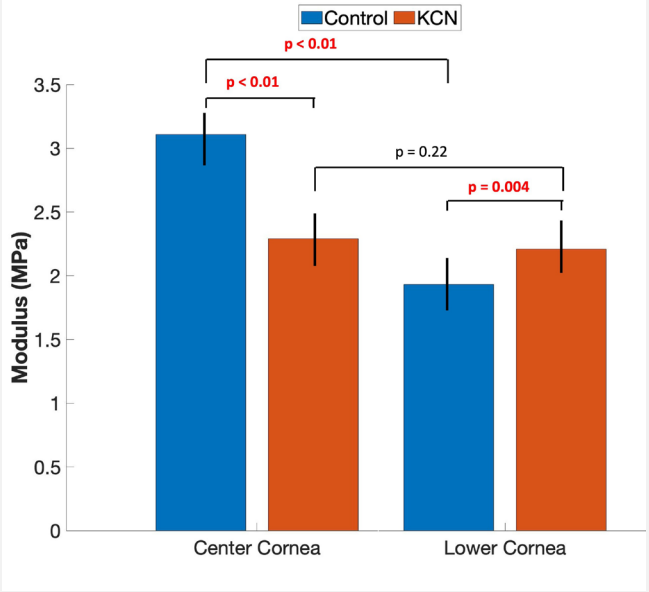

Figure 3: Average modulus for control central corneas and central corneas from stages I, II, III and IV KC subjects. The average modulus for control central corneas was found to be 3.1±0.31 MPa while that for KC central corneas was 2.4±0.25 MPa. The average moduli for control central cornea and KC central cornea were statistically different with a p value of <0.01. The average modulus value of inferior central controls and KC corneas were 1.9+/-0.37 and 2.24+/-0.44 MPa, respectively and were statistically different. The average moduli of the central and lower KC corneas were not statistically different. In comparison the moduli of control central and inferior corneas were statistically different.

Figure 5 compares the average normalized weighted displacement versus frequency plots of inferior control and KC corneas. This Figure illustrates that the 140 and 240-250 Hz peaks are significantly different in the inferior corneas of control and KC eyes. The modulus of the inferior corneas from controls and KC subjects calculated from resonant frequency VOCT measurements were determined using VOCT results and equation 1 are shown in Figure 4.

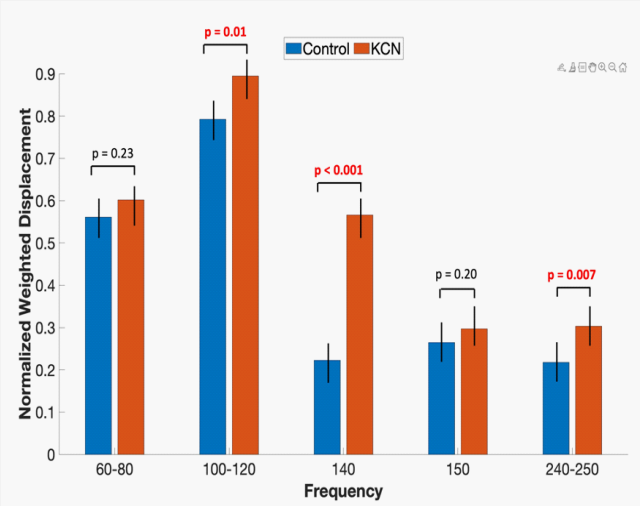

Figure 4: Normalized average weighted displacement versus frequency for control inferior cornea and inferior cornea from subjects with stages I, II, III, and IV KC. Note significant differences in control and KC inferior corneas were observed in the 140 and 240-250 Hz peaks.

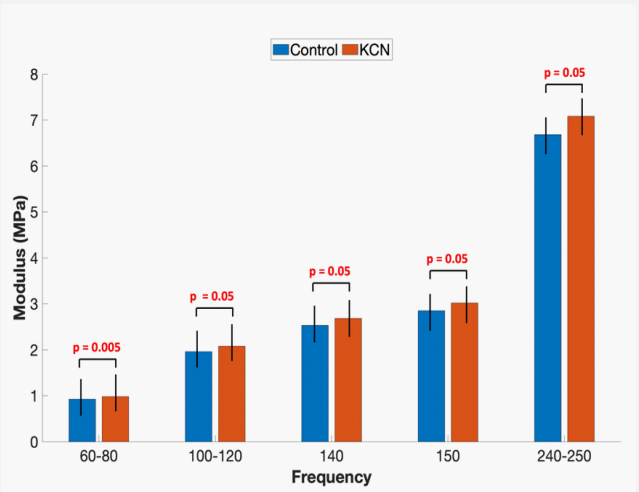

Figure 5: The modulus of the different components of inferior corneas from controls and inferior corneas from KC subjects calculated from resonant frequency measurements on corneal components (Figure 2) determined using VOCT and using equation 1. Note the significant differences between the moduli of the components of controls and KC subjects. There are large differences in the peak heights seen in Figure 4. KC inferior corneal components were stiffer than controls.

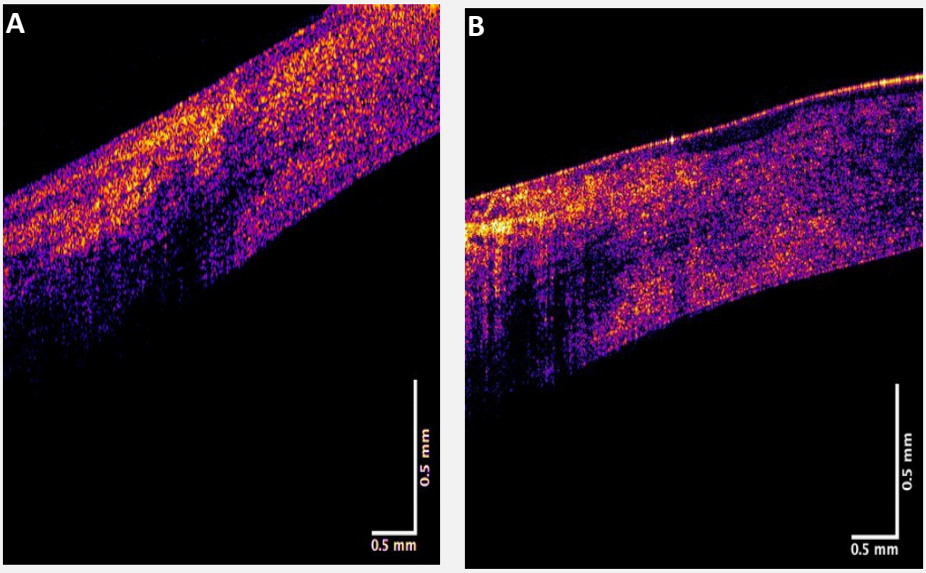

Figure 6: Color-coded OCT images of the corneal-limbus interface illustrating the apparent change in connections between corneal and limbus collagen fibrils in KC in the inferior cornea. (A) Corneal-limbus interface in control cornea and (B) the corneal-limbus interface in a subject with stage III KC. The connection of the collagen fibrils in A is different than that in the KC cornea shown in B indicating a possible change in collagen fibril diameters and amount. A space and perhaps the location of slippage of the connections between the KC limbus and corneal collagen fibrils. This site may serve as the location where slippage occurs that leads to cone formation at a point away from the limbus in the central and paracentral region where the curvature and stress is greatest.

Figure 3 compares the average modulus of the inferior cornea for controls and KC patients with stages I, II, III and IV KC. The average values of the central and inferior cornea moduli of KC corneas are not statistically different. The distribution of the components in the inferior cornea is different between control and KC patients (Figure 4). Figure 3 also shows that the average modulus for lower control corneas and those from stages I, II, III and IV keratoconus subjects calculated using the data in Figures 4 and 5 are different. KC inferior cornea component modulus values are stiffer than the modulus values of the inferior cornea controls. The average modulus was calculated by weighting using the amount of reflected light (peak heights) for each component in making this calculation. The average corneal moduli for inferior control and KC corneas are 1.9±0.37 MPa and 2.24±0.44 MPa, respectively. These moduli are statistically different suggesting that more stiffer collagen components are present in the lower KC corneas compared to the controls (Figures 4 and 5). A modulus of about 2.45 MPa has been reported for dermal collagen in skin and in blood vessels using VOCT [24-26] suggesting that changes in the elastic modulus of KC corneas reflect changes in the collagen component content of KC inferior corneas. The p value for comparing the average modulus of lower

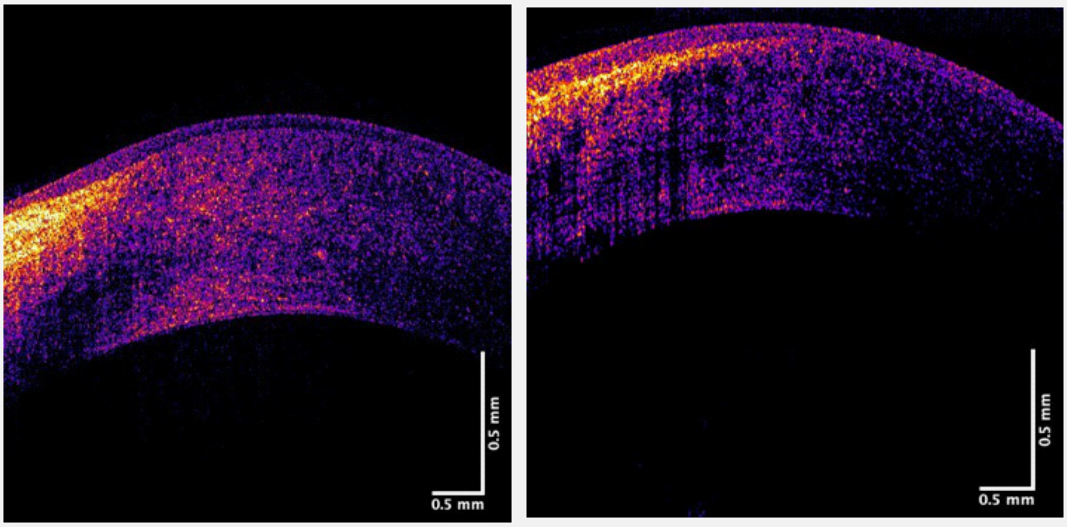

Figure 7: Color-coded OCT image of inferior cornea showing limbus-corneal junction of a control (left) and the junction of a KC stage III patient (right). The apparent thickening of the epithelial layer ratio in a stage III KC cornea at the cornea-limbus interface is statistically significant as shown in Figure 8.

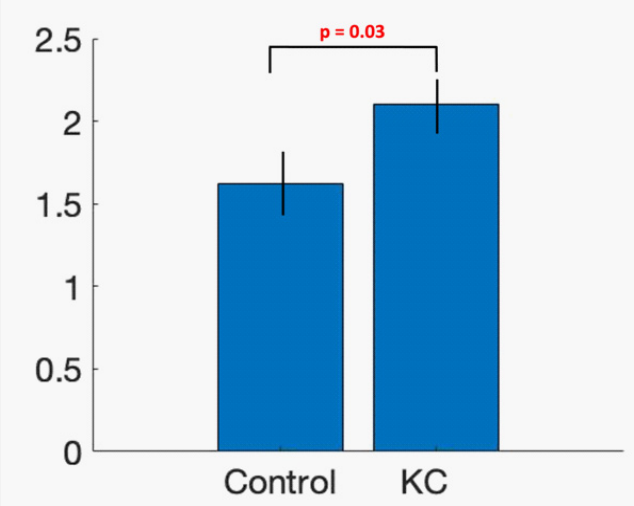

Figure 8: A plot of the average thickness ratio calculated as the ratio of epithelial thickness measured at the limbus divided by the thinnest epithelium thickness measured in the inferior cornea. The limbus thickness was calculated from the OCT images for control and the KC corneas.

control and central corneas of KC patients is 0.0004 indicates that KC patients have increased inferior corneal stiffness.

Color-coded OCT images of the inferior corneal-limbus interface in a control and a stage III subject are shown in Figure 6. These images suggest that in the control the collagen fibrils at the interface with the inferior cornea near the limbus appear different (Figure 7A) than in the KC cornea (Figure 6B). The vertical arrow shown in Figure 4B marks the formation of a space that is seen to form in the KC cornea between the epithelium and the lamellae. This space along with the changes in the KC limbus and cornea collagen fibrils (140 Hz and 240-250 Hz peaks) may reflect increased synthesis and slippage of the cornea collagen fibrils. The location of the thinness point in the cornea where cone formation occurs is away from the limbus in KC suggesting that tensile forces exerted on the cornea at the central and paracentral regions promote further cone formation and thinning by lamellar slippage.

Figure 8 shows a plot of the thickness ratio in the inferior cornea calculated as the ratio of epithelial thickness measured at the limbus divided by the thinnest epithelium thickness. This plot shows that the ratio of corneal thicknesses for KC subjects is larger than for controls and the results are significant at a p value of 0.03.

The thinnest epithelium thickness was calculated from inferior cornea OCT images. Multiple epithelium thickness measurements were made at different points along the inferior cornea and the thinnest measurement was recorded for calculation of the ratio.

Machine learning results

VOCT results and machine learning were used to differentiate controls from stages I and II KC. The sensitivity and specificity were calculated using Equations 1 and 2. Table 2 shows a comparison of the sensitivity and specificity used to differentiate resonant frequency peak heights in controls and all KC corneas seen in Figures 1 and 4 based on machine learning analysis. The results shown in Tables 2 and 3 indicate that the sensitivity and specificity calculations were able to differentiate between control central and inferior corneas from KC subjects using the VOCT peaks shown in Figures 1 and 5.

Table 2: Sensitivity and specificity of differentiating between controls and different KC stages based on resonant frequency peak heights using a logistic regression model.

Central cornea.	**Control vs Stages I & II**	**Control vs Stages I, II, III & IV**
Sensitivity	100%	100%
Specificity	100%	100%
AUC	1.0	1.0
Inferior cornea	**Control vs Stages I & II**	**Control vs Stages I, II, III & IV**
Sensitivity	92.8%	92.3%
Specificity	100%	92.3%
AUC	0.96	0.97

Table 3: Use of machine learning and resonant frequency peak heights to differentiate normal central corneas from corneas of stages I, II, III and IV KC subjects using the logistic regression model. The results suggest that the differences in the 140-150 and 240-250 Hz peak heights can be used to differentiate between normal and KC corneas 100% of the time.

Frequency	% Accuracy for center cornea*	% Accuracy for inferior cornea*
60-80 Hz	82.4%	100%
110-120 Hz	52.9%	52.9%
140-150Hz	100%	100%
240-250 Hz	100%	100%

Machine Learning algorithm run on specific frequencies – only accuracy (Equation 3) could be calculated at these specific frequencies

Discussion

We have used a new technique termed VOCT to identify the changes in biomechanical properties that are associated with the onset of keratoconus. The biomechanical properties of human and animal corneas have been the subject of numerous research studies, many of which conclude that the KC corneas are softer than control normal corneas. KC is a corneal disease characterized by thinning and steepening of the cornea [7]. Progressive stromal thinning, rupture of the anterior limiting membrane, and subsequent cone formation occurs in the central/paracentral cornea [9]. Progressive corneal thinning results in corneal protrusion and cone formation [11-13]. The KC cornea assumes a conical shape because of the degeneration of the corneal stromal tissue. Morphological changes in collagen fibers, such as slippage of the layers of collagen fibrils, may explain stromal thinning in KC eyes [12]. Significant changes in various biochemical factors such as collagen, proteoglycans, matrix metalloproteinases, and lysyl oxidase have been reported [17]. It has been hypothesized that biomechanical alterations in KC patients can be detected before morphologic changes. However, biomechanics of KC corneas has been limited by the lack of in vivo measurement techniques and/or devices.

Weighted displacement versus frequency measurements

In this study, VOCT was used to quantitatively define differences in control and KC corneas both in the central and inferior regions. The components associated with the 60-80, 110-120, 140-150, and 240-250 Hz resonant frequency peaks have been assigned previously based on the results of human and porcine corneal studies [1,20-23]. The 60-80 Hz peak is associated with corneal epithelial cells and keratocytes [1,21-23], the 110-120 Hz and 140-150 Hz peaks are associated with the collagen lamellae [1,20-22], and the 240-250 peaks are associated with the limbus [1,20-23]. In this study KC corneas show changes in these peaks in the central cornea with decreases in the 60-80, 150 and 250 Hz peaks and an increase in the 140 Hz peak (see Figure 1). These results are consistent with a loss of cells and a decrease in the amount of collagen in the lamellae and at the limbus-corneal junction centrally. Cone formation is typically observed in the central-paracentral region where the curvature and stress concentration are greatest. These changes are consistent with the largest loss in average modulus occurring in the KC central region as seen in Figure 4. The loss in average modulus in the central KC region is in part compensated by an increase in the average stiffness in the lower KC cornea and an increase in the collagen content of the lamellae and limbus in the inferior cornea based on the increased peak heights of these components (Figure 4). These results suggest that the average stiffness of the central and lower corneas appear to be identical in KC and that the loss of average central corneal stiffness is offset by an increased collagen synthesis in the inferior cornea with an associated average increase in stiffness compared to controls.

OCT images of normal and KC corneas

A change in the structure of the inferior limbus-corneal junction is associated with the increased average stiffness of the lower KC cornea with respect to controls. As shown in Figures 7 and 8, in a stage III KC patient a change appears to develop at the lower limbus-corneal junction where the epithelium appears to separate from the underlying stroma. The ratio of the inferior epithelial thickness at the limbus divided by the thickness at the thinnest point on the inferior cornea is statistically greater for KC subjects for different stages compared to controls that compensates for this change as is shown in Figure 9. This suggests that collagen production (140-150 and 240-250 Hz peaks, Figure 4) is increased in the inferior cornea resulting in an increase in inferior cornea average modulus (Figure 3) due to changes that occur at the limbus-corneal junction.

Preliminary machine learning

In this pilot study we conducted machine learning using a logistic regression analysis to determine whether it is possible to differentiate control from KC corneas using VOCT data. One limitation was that the number of subjects used in the study in the KC group was small. Using 75% of the data for training the preliminary results in Tables 2 and 3 indicate that differences in the 140-150 and 240-250 Hz peaks can be used to differentiate between controls and stages I, II, III, and IV KC corneas with a high sensitivity and specificity. The agreement between the machine learning results and the statistical analysis of the VOCT data suggest that KC corneas can be differentiated from controls based on the changes in collagen deposition at the limbus-corneal interface and in the collagen lamellae. These results also suggest that characterization of the cornea using a single modulus is misleading since the corneal stiffness varies between the central and inferior regions. In both the central and inferior KC corneas, stiffness changes with respect to controls reflect component composition changes. These changes may result from stress concentration, inflammation, and biosynthetic activity that results in differences in collagen turnover in the central and lower parts of the KC cornea. Further studies are needed to better understand the pathogenesis of KC to provide for early detection clinically before changes in collagen deposition cause changes in the average modulus of the central and inferior cornea leading to cone formation.

Changes in collagen and PGs in KC

A potential explanation of increased collagen stiffness in the inferior cornea KC corneas is reduced interfibrillar distance between Collagen Fibrils (CFs). Studies have reported a significantly shorter interfibrillar distance in the anterior, middle, and posterior stroma in KC corneas compared to normal corneas [11,16]. An increase in CF density and area fraction in severe keratoconus was also shown [11]. The increased packing density in CFs in keratoconus eyes could create a higher modulus value in these pathological corneas. Changes in Proteoglycan (PG) density and type have been observed in KC corneas. KC corneas have significantly higher PG density in all layers studied (anterior, middle, and posterior stroma) compared to normal

eyes [11,16,27], and the PG area fraction was also shown to increase as corneas with ectasia [27]. This could directly influence corneal biomechanics and consequently increase the modulus value. The increased deposition of PGs with sulfated chains in keratoconus may also lead to altered corneal biomechanics [28].

The experimentally observed stiffening of inferior regions of keratoconus corneas may be a compensation mechanism to reduce corneal topographical changes and slippage of collagen fibrils. Rapid corneal curvature changes might otherwise lead to catastrophic corneal failure because of increased stress concentrations that are associated with increased corneal curvature

Limitations to this pilot study include the limited number of KC subject eyes used as well as the use of 10 Hz intervals in studying the resonant frequency of individual corneal components. The calculation of the average modulus is weighted towards the higher molecular weight components and therefore is a weigh average as opposed to a number average.

Conclusions

In vivo pilot VOCT studies comparing control corneas to corneas from KC patients suggest that changes are observed in the collagen deposited in the limbus and lamellae that lead to changes in average stiffness in the central and inferior corneas. VOCT and machine learning results are consistent with the largest loss in modulus occurring in the KC central/paracentral region. The loss in modulus in the central/paracentral KC region is in part compensated by an increase in the stiffness in the lower KC cornea and an increase in the collagen content of the inferior corneal lamellae and limbus. The results suggest that the average stiffness of the central and lower KC corneas appear to be similar and that any loss in central corneal stiffness in KC is offset by an increase in the stiffness of the inferior cornea. However, due to the increased curvature of the central cornea compared to the inferior cornea, increased stress concentration in the central corneal region leads to cone formation at the point of maximum curvature which is typically located centrally/paracentrally.

The results of the machine learning studies indicate that differences in the 140-150 and 240-250 Hz peaks can be used to differentiate between controls and stages I, II, III, and IV KC corneas with a high sensitivity and specificity. Determination of the exact sensitivity and specificity for each stage will require additional data on KC subjects. Stage analysis of the VOCT resonant frequency data suggest that KC corneas can be clinically identified using VOCT.

References

1. Silver FH, Deshmukh T, Benedetto D, Gonzalez-Mercedes M. Dynamic Ocular Response to Mechanical Loading: The Role of Viscoelasticity in Energy Dissipation by the Cornea. Biomimetics. 2023; 8: 63.
2. Silver FH, Freeman JW, Gurinder GP. Collagen self-assembly and the development of tendon mechanical properties. J. Biomech. 2003; 36: 1529-1553.
3. Horvath I, Foran D, Silver FH. Energy Analysis of Flow Induced Harmonic Motion in Blood Vessel Walls. Cardiovasc. Eng. 2005; 5: 21-28.
4. Silver FH, Kelkar N, Deshmukh T. Molecular Basis for Mechanical Properties of ECMs: Proposed Role of Fibrillar Collagen and Proteoglycans in Tissue Biomechanics. Biomolecules. 2021; 11: 1018.
5. Silver FH, Siperko LM. Mechanosensing and Mechanochemical Transduction: How Is Mechanical Energy Sensed and Converted into Chemical Energy in an Extracellular Matrix? Crit. Rev. Biomed. Eng. 2003; 31: 255-331.
6. Silver FH, Deshmukh T, Benedetto D, Gonzalez-Mercedes M, Mesica A. Measurement of the Elastic Modulus of Cornea, Sclera and Limbus: The Importance of the Corneal-Limbus-Scleral Biomechanical Unit. Front. Biosci. (Schol Ed). 2022; 14: 30.
7. Khaled ML, Helwa I, Drewry M, Seremwe M, Estes A, et al. Molecular and Histopathological Changes Associated with Keratoconus. BioMed Research International. 2017; 7803029: 16.
8. Claessens JLJ, Godefrooij DJ, Vink G, Frank LE, Robert P L Wisse, et al. Nationwide epidemiological approach to identify associations between keratoconus and immune mediated diseases. Br J Ophthalmol. 2022; 106: 1350-1354.
9. Santodomingo-Rubido J, Carracedo G, Asaki Suzaki A, Villa-Collar C, Vincent SJ, et al. 2022 Keratoconus: An updated review. Contact Lens and Anterior Eye. 2022; 45: 101559.
10. Sarezky D, Orlin SE, Pan W, Vabder Beek BJ. Trends in Corneal Transplantation in Keratoconus. Cornea. 2017; 36: 131-137.
11. Akhtar S, Bron AJ, Sachin M, Salvi NR, Hawksworth NR, et al. Ultrastructural analysis of collagen fibrils and proteoglycans in keratoconus. Acta Ophthalmol. 2008; 86: 764-772.
12. Meek KM, Tuft SJ, Huang Y, Gill PS, Hayes S, et al. Changes in Collagen Orientation and Distribution in Keratoconus Corneas. Invest Ophthalmol Vis Sci. 2005; 46: 1948 -1956.
13. Vellara HR, Patel DV. Biomechanical properties of the keratoconic cornea: A review. Clin Exp Optom. 2015; 98(1): 31-8. doi: 10.1111/cxo.12211. PMID: 25545947.
14. Nanderan M, Jahanrad A, Balali S. Histopathologic findings of keratoconus corneas underwent penetrating keratoplasty according to topographic measurements and keratoconus severity. Int J Ophthalmol. 2017; 10: 1640-1646.
15. Zhou HY, Cao Y, Wu J, Zhang WS. Role of corneal collagen fibrils in corneal disorders and related pathological conditions. Int J Ophthalmol. 2017; 10: 803-811.
16. Alkanaan A, Barsotti R Kirat O, Khan A, Almubrad T, et al. Collagen fibrils and proteoglycans of peripheral and central stroma of the keratoconus cornea - Ultrastructure and 3D transmission electron tomography. Nature Scientific Reports. 2019; 9: 19963.
17. Shetty R, D'Souza S, Khamar P, Ghosh A, Nuijts RMMA, et al. Biochemical markers and alterations in keratoconus. Asia Pac J Ophthalmol (Phila). 2020; 9: 533-40.
18. Koh S, Inoue R, Ambrósio R, Maeda N, Miki A, et al. Correlation between corneal biomechanical indices and the severity of keratoconus. Cornea. 2020; 39: 215-221.
19. Sinha Roy A, Shetty R, Kummelil MK. Keratoconus. A biomechanical perspective on loss of corneal stiffness. Indian J Ophthalmol. 2013; 61: 392-393.
20. Crespo MA, Jimenez HJ, Deshmukh T, Pulido JS, Saad AS, et al. In Vivo Determination of the Human Corneal Elastic Modulus Using Vibrational Optical Coherence Tomography. Translational Vision Science & Technology. 2022; 11: 11.
21. Daher ND, Saad AS, Jimenez HJ, et al. Identification of the vibrational optical coherence tomography corneal cellular peak. Transl Vis Sci Technol. 2023; 12: 11.
22. Shah RG, Silver FH. Viscoelastic behavior of tissues and implant

materials: Estimation of the elastic modulus and viscous contribution using optical coherence tomography and vibrational analysis. Journal of Biomedical Technology and Research. 2017; 3: 105-109.

23. Silver FH, Shah RG. Mechanical Analysis of Multi-Component Tissues. World Journal of Mechanics. 2017; 7: 121-132.

24. Silver FH, Kelkar N, Deshmukh T. Molecular Basis for Mechanical Properties of ECMs: Proposed Role of Fibrillar Collagen and Proteoglycans in Tissue Biomechanics. Biomolecules. 2021; 11: 1018.

25. Silver FH, Deshmukh T, Gonzalez-Mercedes M. Use of Vibrational Optical Coherence Tomography to Noninvasively Differentiate Between Benign Fibrotic Tissue and Fibrosis Associated with Melanoma, 21st Century Pathology. 2023; 3: 139.

26. Shah RG, DeVore D, Silver FH. Biomechanical analysis of decellularized dermis and skin: Initial in vivo observations using optical cohesion tomography and vibrational analysis. J Biomed Mater Res A. 2018; 106: 1421-1427.

27. Akhtar S, Bron AJ, Salvi S, Hawksworth NR, Tuft SJ, et al. Ultrastructural analysis of collagen fibrils and proteoglycans in keratoconus. Acta Ophthalmol. 2008; 86: 764-72.

28. Funderburgh JL, Hevelone ND, Roth MR, et al. Decorin and biglycan of normal and pathologic human corneas. Invest Ophthalmol Vis Sci. 1998; 39: 1957-1964.

29. Meek KM, Tuft SJ, Huang Y, Gill PS, Hayes S, et al. Changes in Collagen Orientation and Distribution in Keratoconus Corneas. Invest Ophthalmol Vis Sci. 2005; 46: 1948 -1956.